EventUPS: Uncalibrated Photometric Stereo Using an Event Camera

Supplementary Material

Jinxiu Liang[1,2,3#] Bohan Yu[1,2#] Siqi Yang[1,2,4] Haotian Zhuang[5]
Jieji Ren[6] Peiqi Duan[1,2] Boxin Shi[1,2*]

[1] State Key Laboratory of Multimedia Information Processing, School of Computer Science, Peking University
[2] National Engineering Research Center of Visual Technology, School of Computer Science, Peking University
[3] National Institute of Informatics [4] Institute for Artificial Intelligence, Peking University
[5] Tsinghua University [6] Shanghai Jiaotong University
cssherryliang@gmail.com,{ybh1998,yousiki,duanqi0001,shiboxin}@pku.edu.cn,
zht23@mails.tsinghua.edu.cn,jiejiren@sjtu.edu.cn

6. Proof of GBR Resolving

We demonstrate that a lighting system with known 3D structure, defined by its 3D light positions, can resolve the GBR ambiguity up to the classic convex/concave reflection, provided certain generic conditions on the light positions are met.

Theorem 1. *Let P be a set of at least seven light source positions in $\mathbb{R}^3$, represented in homogeneous coordinates as $\mathbf{p} = [x, y, z, 1]^\top$. The corresponding light vector for each source is $\mathbf{s} = u \cdot [x, y, z]^\top$, where $u > 0$ is a light-specific scalar. Suppose the following relation holds for every $\mathbf{p} \in P$:*

$$\begin{bmatrix} v \cdot \mathbf{Gs} \\ 1 \end{bmatrix} = \begin{bmatrix} \mathbf{R} & \mathbf{t} \\ \mathbf{0}^\top & 1 \end{bmatrix} \mathbf{p}$$

where:

1. *$v \neq 0$ is a scalar that may vary for each light source.*
2. *$\boldsymbol{R}$ is a 3×3 orthogonal matrix ($\boldsymbol{R} \in O(3)$, $\det \boldsymbol{R} = \pm 1$) and $\mathbf{t}$ is a 3×1 translation vector.*
3. *$\mathbf{G}$ is a 3×3 GBR transformation matrix:*

$$\mathbf{G} = \begin{bmatrix} 1 & 0 & 0 \\ 0 & 1 & 0 \\ m & n & p \end{bmatrix}.$$

4. *The set P is in general position, meaning the points do not all lie on any quadric surface passing through the origin with equation:*

$$\pi_1 x^2 + \pi_2 xy + \pi_3 xz + \pi_4 x + \pi_5 y^2 + \pi_6 yz + \pi_7 y = 0$$

where not all π_i are zero.

Under these conditions, the only solutions for $\mathbf{t}$ is $\mathbf{t} = \mathbf{0}$, and the only solutions for $(\mathbf{R}, \mathbf{G})$ are the four coupled pairs:

- $(\mathbf{R}, \mathbf{G}) = (\mathrm{diag}(1, 1, 1), \mathrm{diag}(1, 1, 1))$,
- $(\mathbf{R}, \mathbf{G}) = (\mathrm{diag}(1, 1, -1), \mathrm{diag}(1, 1, -1))$,
- $(\mathbf{R}, \mathbf{G}) = (\mathrm{diag}(-1, -1, 1), \mathrm{diag}(1, 1, -1))$,
- $(\mathbf{R}, \mathbf{G}) = (\mathrm{diag}(-1, -1, -1), \mathrm{diag}(1, 1, 1))$.

Remark. *A common physical constraint in photometric stereo is that the lights must remain in the same hemisphere relative to the scene (*i.e.*, always in front of the camera, $z > 0$). This implies that the z-component of a light's position must have the same sign in both the true and ambiguous configurations. This prunes the four solutions to two: the first and the third solutions.*

Proof. Let $\mathbf{R} = \begin{bmatrix} a & d & g \\ b & e & h \\ c & f & i \end{bmatrix}$ and $\mathbf{t} = \begin{bmatrix} j \\ k \\ l \end{bmatrix}$.

For a point $\mathbf{p} = [x, y, z, 1]^\top$, the left-hand side becomes:

$$\mathbf{Gs} = u \begin{bmatrix} 1 & 0 & 0 \\ 0 & 1 & 0 \\ m & n & p \end{bmatrix} \begin{bmatrix} x \\ y \\ z \end{bmatrix} = u \begin{bmatrix} x \\ y \\ mx + ny + pz \end{bmatrix}.$$

Thus:

$$\begin{bmatrix} v \cdot \mathbf{Gs} \\ 1 \end{bmatrix} = [vux, vuy, vu(mx + ny + pz), 1]^\top.$$

The right-hand side gives:

$$\begin{bmatrix} \mathbf{R} & \mathbf{t} \\ \mathbf{0}^\top & 1 \end{bmatrix} = \begin{bmatrix} a & d & g & j \\ b & e & h & k \\ c & f & i & l \\ 0 & 0 & 0 & 1 \end{bmatrix} \begin{bmatrix} x \\ y \\ z \\ 1 \end{bmatrix} =$$

$$[xa + yd + zg + j, xb + ye + zh + k, xc + yf + zi + l, 1]^\top.$$

Equating the vector components of both sides gives three

#Equal contributions. *Corresponding author.

scalar equations that must hold for each point in P:

$$vux = xa + yd + zg + j, \quad (18)$$
$$vuy = xb + ye + zh + k, \quad (19)$$
$$vu(mx + ny + pz) = xc + yf + zi + l. \quad (20)$$

The scalar vu varies with each light source and must be eliminated to obtain constraints on the matrices. We can isolate vu from (18) and (19) (assuming at least one point has $x \neq 0$ and $y \neq 0$, which is guaranteed by the general position condition) by cross-multiplication. From equations (18) and (19), multiplying (18) by y and (19) by x:

$$vuxy = y(xa + yd + zg + j),$$
$$vuxy = x(xb + ye + zh + k).$$

Equating the right-hand sides:

$$y(xa + yd + zg + j) = x(xb + ye + zh + k).$$

Rearranging the terms produces the equation of a quadric surface:

$$bx^2 + (e - a)xy + hxz + kx - dy^2 - gyz - jy = 0. \quad (21)$$

This equation holds for every point in P and passes through the origin $(0, 0, 0)$ (substituting $x = y = z = 0$ yields $0 = 0$).

Note that this quadric has a special form: it contains no z^2 or standalone z terms, which is a direct consequence of our elimination process.

By the theorem's premise, the derived quadric (21) is precisely of the form excluded by the general position condition. The vector of its coefficients is $\boldsymbol{\pi} = [b, e - a, h, k, -d, -g, -j]^\top$. For each point $\mathbf{p}_i = [x_i, y_i, z_i, 1]^\top \in P$, we obtain a linear constraint:

$$[x_i^2, x_i y_i, x_i z_i, x_i, y_i^2, y_i z_i, y_i]\boldsymbol{\pi} = 0.$$

Stacking these constraints for seven points yields the homogeneous system $\mathbf{M}\boldsymbol{\pi} = \mathbf{0}$, where $\mathbf{M}$ is a 7×7 matrix with rows $[x_i^2, x_i y_i, x_i z_i, x_i, y_i^2, y_i z_i, y_i]$.

Since the seven or more points in P do not lie on such a surface (unless it is trivial), the coefficients must all be zero, *i.e.*, $\boldsymbol{\pi} = \mathbf{0}$, therefore,

$$b = 0, e - a = 0, h = 0, k = 0, d = 0, g = 0, j = 0.$$

This simplifies our matrices to:

$$\mathbf{R} = \begin{bmatrix} a & 0 & 0 \\ 0 & a & 0 \\ c & f & i \end{bmatrix}, \quad \mathbf{t} = \begin{bmatrix} 0 \\ 0 \\ l \end{bmatrix}.$$

Since $\boldsymbol{R} \in O(3)$ is orthogonal, we have $\mathbf{R}^\top\mathbf{R} = \mathbf{I}_3$. Computing the rows: Row 1: $[a, 0, 0]$ has norm $|a| = 1$, so $a = \pm 1$.

Row 2: $[0, a, 0]$ has norm $|a| = 1$ (confirmed).

Row 3: $[c, f, i]$ must have unit norm and be orthogonal to rows 1 and 2:

- Orthogonality conditions:
  - With row 1: $ac + 0 \cdot f + 0 \cdot i = 0 \Rightarrow c = 0$ (since $a \neq 0$).
  - With row 2: $0 \cdot c + af + 0 \cdot i = 0 \Rightarrow f = 0$ (since $a \neq 0$).
- Unit norm constraint: $c^2 + f^2 + i^2 = 0^2 + 0^2 + i^2 = 1 \Rightarrow i = \pm 1$.

Therefore: $\mathbf{R} = \mathrm{diag}(a, a, i)$ where $a, i \in \{-1, 1\}$.

Now we use the simplified forms of $\mathbf{R}$ and $\mathbf{t}$ in the initial scalar equations. From equation (18) with $d = g = j = 0$: $vux = ax$.

This yields $vu = a$ for points with $x \neq 0$ or $y \neq 0$. Substituting $vu = a$, $c = f = 0$, and the simplified $\mathbf{R}$ into equation (20):

$$a(mx + ny + pz) = zi + l.$$

Rearranging gives the equation of a plane:

$$amx + any + (ap - i)z - l = 0.$$

This equation must hold for all points in P. However, the points in P cannot be coplanar. If they were, they would lie on a plane $Ax + By + Cz + D = 0$. This would imply they also lie on the quadric surface defined by $x(Ax + By + Cz + D) = Ax^2 + Bxy + Cxz + Dx = 0$, which is one of the forms forbidden by the general position condition.

Since the points are not coplanar, the only way the planar equation can hold for all of them is if all its coefficients are zero:

- $am = 0 \implies m = 0$ (since $a \neq 0$),
- $an = 0 \implies n = 0$ (since $a \neq 0$),
- $ap - i = 0 \implies p = i/a = ia$ (since $a^2 = 1$),
- $-l = 0 \implies l = 0$.

For points with $x = y = 0$ (if any), consistency is verified after deriving the coefficients: substituting into (20) gives $vup = i + l/z$, but after zeroing coefficients ($m = n = 0$, $p = ia$, $l = 0$), we obtain $vu = a$, consistent with other regions.

This fully determines the parameters of $\mathbf{G} = \mathrm{diag}(1, 1, ai)$ and $\mathbf{t} = \mathbf{0}$.

We have $\mathbf{R} = \mathrm{diag}(a, a, i)$ and $\mathbf{G} = \mathrm{diag}(1, 1, ai)$ where $a, i \in \{-1, 1\}$.

The four possibilities are:

- $(a, i) = (1, 1)$: $\mathbf{R} = \mathrm{diag}(1, 1, 1)$, $\mathbf{G} = \mathrm{diag}(1, 1, 1)$,
- $(a, i) = (1, -1)$: $\mathbf{R} = \mathrm{diag}(1, 1, -1)$, $\mathbf{G} = \mathrm{diag}(1, 1, -1)$,
- $(a, i) = (-1, 1)$: $\mathbf{R} = \mathrm{diag}(-1, -1, 1)$, $\mathbf{G} = \mathrm{diag}(1, 1, -1)$,
- $(a, i) = (-1, -1)$: $\mathbf{R} = \mathrm{diag}(-1, -1, -1)$, $\mathbf{G} = \mathrm{diag}(1, 1, 1)$.

Existence of general position point sets.

To ensure the theorem is not vacuous, we must show that a set of points P satisfying the general position condition exists. The condition requires that the only solution to $\mathbf{M}\boldsymbol{\pi} = \mathbf{0}$ is $\boldsymbol{\pi} = \mathbf{0}$, where $\mathbf{M}$ is the 7×7 matrix whose rows are $[x_i^2, x_i y_i, x_i z_i, x_i, y_i^2, y_i z_i, y_i]$ for the seven points. This is equivalent to showing that we can find 7 points such that $\mathbf{M}$ is invertible.

We can construct such a set:

1. Choose 5 points on the plane $z = z_0$ (with $z_0 \neq 0$). Let their (x, y) coordinates be five points on a circle that does not pass through the origin. Let $\boldsymbol{\pi} = [\pi_1, \ldots, \pi_7]^\top$ be the coefficient vector of the forbidden quadric. On this plane, any quadric of our form becomes:

$$\pi_1 x^2 + \pi_2 xy + \pi_5 y^2 + (\pi_3 z_0 + \pi_4)x + (\pi_6 z_0 + \pi_7)y = 0.$$

   This is a conic section in the xy-plane passing through the origin. However, five points uniquely define a conic. The unique conic passing through our five chosen points is the circle we constructed, which does not pass through the origin. This is a contradiction unless all the coefficients of the conic are zero. Therefore:

$$\begin{aligned} &\pi_1 = \pi_2 = \pi_5 = 0, \\ &\pi_3 z_0 + \pi_4 = 0 \implies \pi_4 = -\pi_3 z_0, \\ &\pi_6 z_0 + \pi_7 = 0 \implies \pi_7 = -\pi_6 z_0. \end{aligned}$$

   This means that for any quadric of the forbidden form to pass through these five points, its equation must simplify to: $\pi_3 xz - \pi_3 z_0 x + \pi_6 yz - \pi_6 z_0 y = 0$, which can be factored as $(\pi_3 x + \pi_6 y)(z - z_0) = 0$. This is satisfied for our first five points, as $z - z_0 = 0$.
2. Choose 2 additional points, $\mathbf{p}_6$ and $\mathbf{p}_7$, on a different plane (e.g., $z = z_1$, where $z_1 \neq z_0$ and $z_1 \neq 0$). For these points, $z - z_0 \neq 0$, so the equation reduces to $\pi_3 x + \pi_6 y = 0$:

$$\begin{aligned} \pi_3 x_6 + \pi_6 y_6 = 0, \\ \pi_3 x_7 + \pi_6 y_7 = 0. \end{aligned}$$

   We can choose $\mathbf{p}_6$ and $\mathbf{p}_7$ such that their projection vectors $[x_6, y_6]^\top$ and $[x_7, y_7]^\top$ are linearly independent (i.e., not collinear and not the zero vector). This ensures that the only solution to the 2×2 system above is the trivial one: $\pi_3 = 0$ and $\pi_6 = 0$. Substituting back, we find $\pi_4 = -\pi_3 z_0 = 0$ and $\pi_7 = -\pi_6 z_0 = 0$.

This construction forces all coefficients $\pi_1, \ldots, \pi_7$ to be zero. Therefore, the only quadric of the specified form passing through these seven points is the trivial one, meaning the points satisfy the general position condition. Such sets exist, and the proof is complete. □

7. More Implementation Details

7.1. Lighting Configurations

We designed two configurations with known relative geometry but unknown global pose to resolve the UPS ambiguity.

Case 1: Coaxial dual-ring lights. This configuration uses two concentric rings of lights with known radii $r_1 > 0$ and $r_2 > 0$ and a known axial separation $\Delta d \neq 0$. The lights' canonical positions in the local frame are:

$$\boldsymbol{p}_i(t) = [r_i \cos t, r_i \sin t, z_i], \tag{22}$$

where $z_1 = 0, z_2 = \Delta d$ denotes the axial offset, and $t \in [0, 2\pi)$ (*e.g.*, equally spaced for M sources) parametrizes the angular position around the ring.

In this system, these points span two parallel planes, encoding depth via differences Δd in lighting directions between rings. Rings are circles centered on the z-axis, not passing through the origin. This mirrors the proof's construction: points on two $z =$ constant planes with circular distributions not through the origin.

We validate it satisfies the general position as follows, drawing on the proof's construction (points on two planes with circles not through origin, extended to non-coplanar sets): Restrict to one plane ($z = 0$); the forbidden quadric becomes a conic in xy passing through $(0, 0)$ (no constant term). With ≥ 5 points on a circle not through $(0, 0)$, the unique conic through them has a constant term, so no matching conic without constant exists unless trivial. Adding points on $z = \Delta d$ forces remaining coefficients to zero (by linear independence of $[x_k, y_k]$). The 3D distribution resolves translations (axial separation fixes z-shift; angular spread fixes xy-shifts). Thus, the general position holds for generic $r_1 \neq r_2, \Delta d \neq 0$, and non-collinear angular positions.

Case 2: Trefoil curve. This configuration uses a single ring of lights mounted on a tilted, rotating mechanism to trace a non-planar, asymmetric 3D trefoil curve. The light positions are defined by:

$$\begin{aligned} \boldsymbol{p}(t) = &\begin{bmatrix} (r_1 + r_2 \sin(\omega t + \phi)\cos(\alpha))\cos(t) \\ (r_1 + r_2 \sin(\omega t + \phi)\cos(\alpha))\sin(t) \\ -r_2 \sin(\omega t + \phi)\sin(\alpha) \end{bmatrix} + \\ &\begin{bmatrix} -r_2 \cos(\omega t + \phi)\sin(t) \\ r_2 \cos(\omega t + \phi)\cos(t) \\ 0 \end{bmatrix} \end{aligned} \tag{23}$$

where r_1, r_2 are radii, α is the tilt angle, ω is a frequency ratio, $t \in [0, 2\pi)$ parametrizes the curve, and ϕ is a phase shift. This structure combines circular motion in the xy-plane (radius r_1) and a secondary oscillation (amplitude r_2, tilt α, frequency ω, phase ϕ) that traces a 3D trefoil

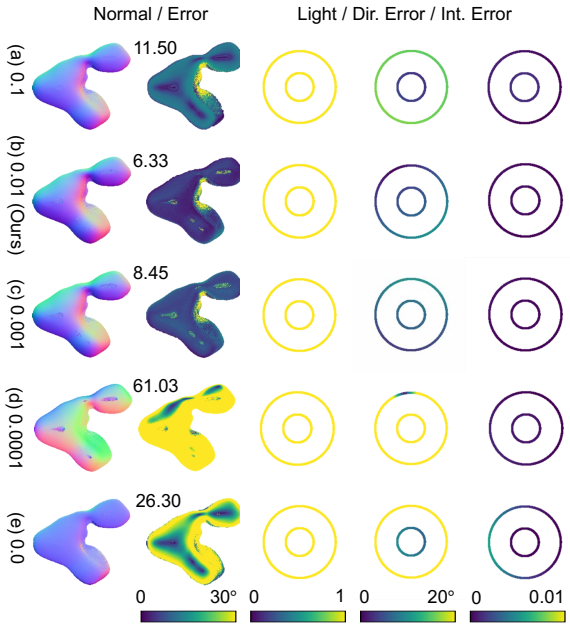

Figure 9. Effectiveness of the integrability constraint. As the weight λ_{int} decreases from (a) 0.1 to (e) 0, the MAE sharply increases. Without this constraint ($\lambda_{\text{int}} = 0$), the solution is ambiguous, leading to errors in both normal and lighting estimation. Our chosen value of (b) $\lambda_{\text{int}} = 0.01$ provides the best balance.

curve. The curve is non-planar (z-component varies with $\sin(\omega t + \phi)$), asymmetric (trefoil pattern breaks rotational symmetry), and spans $\mathbb{R}^3$. Sampled points (≥ 7, equally spaced in t) are in general position if parameters ensure no accidental alignment on low-degree surfaces.

We validate it satisfies the general position as follows: The curve avoids coplanarity (z-variation) and special quadrics. For generic parameters (*e.g.*, $r_1 \neq r_2 > 0$, $\alpha \neq 0$, $\omega \neq 1$, $\phi \neq 0$), sampled points do not satisfy any non-trivial forbidden quadric. This follows from perturbation: start with the proof's construction (non-coplanar points not on such quadrics), and note the trefoil is a continuous deformation preserving genericity. The asymmetry and 3D spread resolve rotations/translations. Numerically, for specific parameters (*e.g.*, $r_1 = 1$, $r_2 = 0.5$, $\alpha = \frac{\pi}{4}$, $\omega = 3$, $\phi = 0$), sampling 7 points yields a full-rank $\boldsymbol{M}$ (verifiable via SVD; rank deficiency would require unlikely parameter tuning). Thus, the general position holds.

Both configurations satisfy the requirements. They are continuous (parameterized by $t \in [0, 2\pi]$), but in practice, ≥ 7 discrete points are placed (equally placed). Both configurations are realizable with off-the-shelf components and are suitable for handheld operation.

7.2. B-Spline Coefficients

For the lighting estimation with continuous representation, we use temporal coefficients $C_{j,l}(t)$ defined by the standard

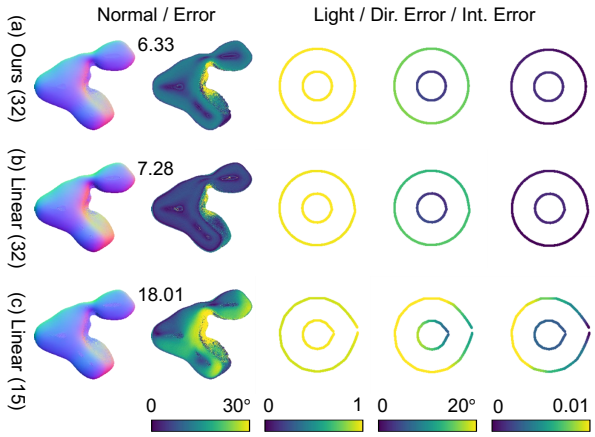

Figure 10. Ablation on continuous lighting representation. We compare (a) our cubic B-spline model with (b, c) a simpler linear interpolation model. Using (b) linear interpolation with the same number of control points (32) results in an increase in error. Reducing the knots to (c) 15 leads to a degradation in performance, as the model can no longer capture the smooth lighting variation.

De Boor–Cox recurrence relation for a spline of order l (degree $l-1$):

$$C_{j,0}(t) = \begin{cases} 1 & \text{if } t_j \leq t < t_{j+1}, \\ 0 & \text{otherwise,} \end{cases} \tag{24}$$

and

$$C_{j,l}(t) = \frac{t - t_j}{l\Delta t} C_{j,l-1}(t) + \frac{t_{j+l+1} - t}{l\Delta t} C_{j+1,l-1}(t). \tag{25}$$

8. Further Analysis and Ablation Studies

Synthetic data generation. To enable comprehensive evaluation, we created a synthetic dataset using objects from the Blobby dataset [15]. For each object, we rendered 500 dense images under rotating lighting conditions for 6 complete rounds, using the dual ring scanning pattern. These images were then converted to event streams using the ESIM simulator [29].

Effectiveness of the integrability constraint. As shown in Fig. 9, the integrability constraint is crucial for resolving ambiguity. Removing it ($\lambda_{\text{int}} = 0$) causes the average MAE to increase by over 18%, demonstrating its effectiveness in pruning incorrect solutions allowed by the GBR ambiguity.

Effectiveness of the continuous lighting representation. We ablated our B-spline model to validate its design. Fig. 10 shows that a cubic spline significantly outperforms linear interpolation, which yields higher MAE with the same number of control points. This validates our choice of a cubic spline representation for handling asynchronous data.

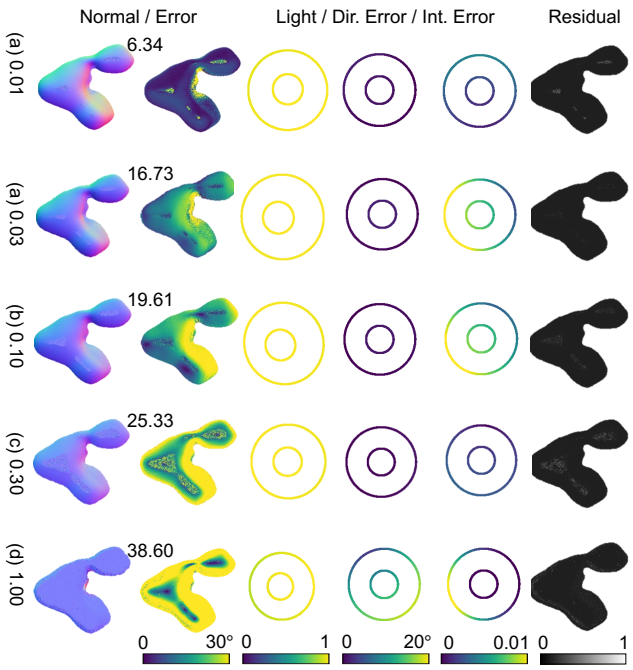

Figure 11. Robustness to ambient illumination. We test our method on synthetic data with varying ratios of ambient to direct illumination. Performance remains stable for ratios up to 0.10, and degrades gracefully thereafter.

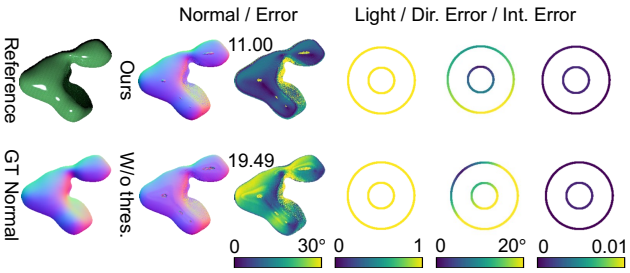

Figure 12. Robustness to specular highlights, a common non-Lambertian effect. Our EventUPS filters high-frequency events that often correspond to specularities. The top row shows the result with filtering, achieving a low MAE. The bottom row shows the result without filtering, where specular events introduce significant artifacts and increase the error.

Robustness to ambient illumination. Fig. 11 demonstrates our method's strong robustness to ambient light—a critical feature for real-world deployment. Our augmented null space formulation explicitly models this effect, allowing EventUPS to maintain high accuracy even when the ambient light is 10% as strong as the direct illumination. Performance degrades gracefully, far surpassing methods that assume dark-room conditions.

Robustness to non-Lambertian effects. Following [45], we filter high-frequency events (often due to specular highlights or sharp shadow boundaries) using thresholding. As shown in Fig. 12, this effectively mitigates artifacts from moderate specular highlights, demonstrating that our method's robustness.

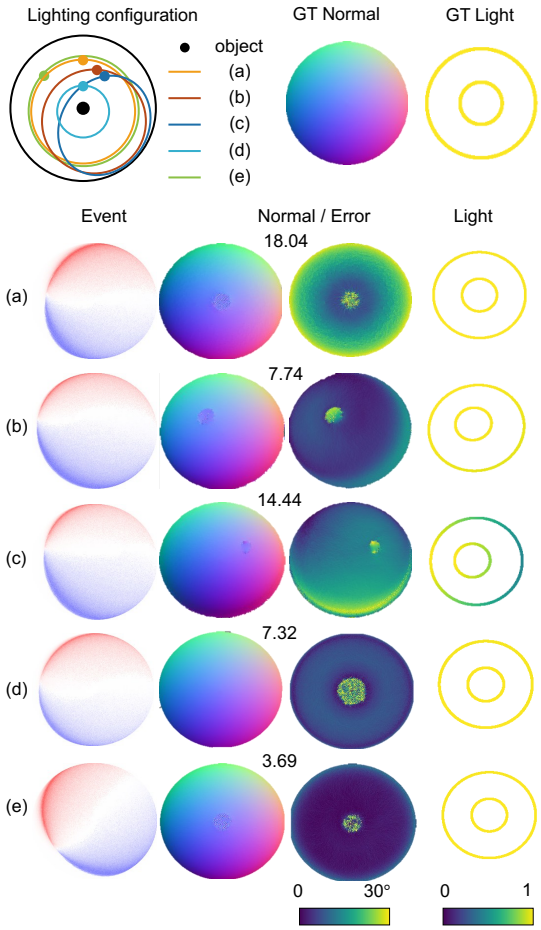

Figure 13. Robustness to the lighting system pose. We simulated various transformations relative to the camera: (a) a view-centered baseline, (b) rotation around the object, (c) rotation about the light's axis, (d) translation along the z-axis, and (e) rotation around the z-axis. The top-left plot shows the projected light path for each case. EventUPS maintains consistent, high-quality performance across all configurations.

Robustness to lighting system pose. Fig. 13 confirms that our method is resilient to the global pose of the lighting system. This robustness is critical for practical use cases, especially handheld operation, where precise alignment is not feasible.

9. Complete Evaluation Results

Complete visual results of our method, EventPS [45], PF14 [28] (56 frames), and CW20 [5] (6 frames) for all objects in the DiLiGenT-Ev dataset are shown in Fig. 14.

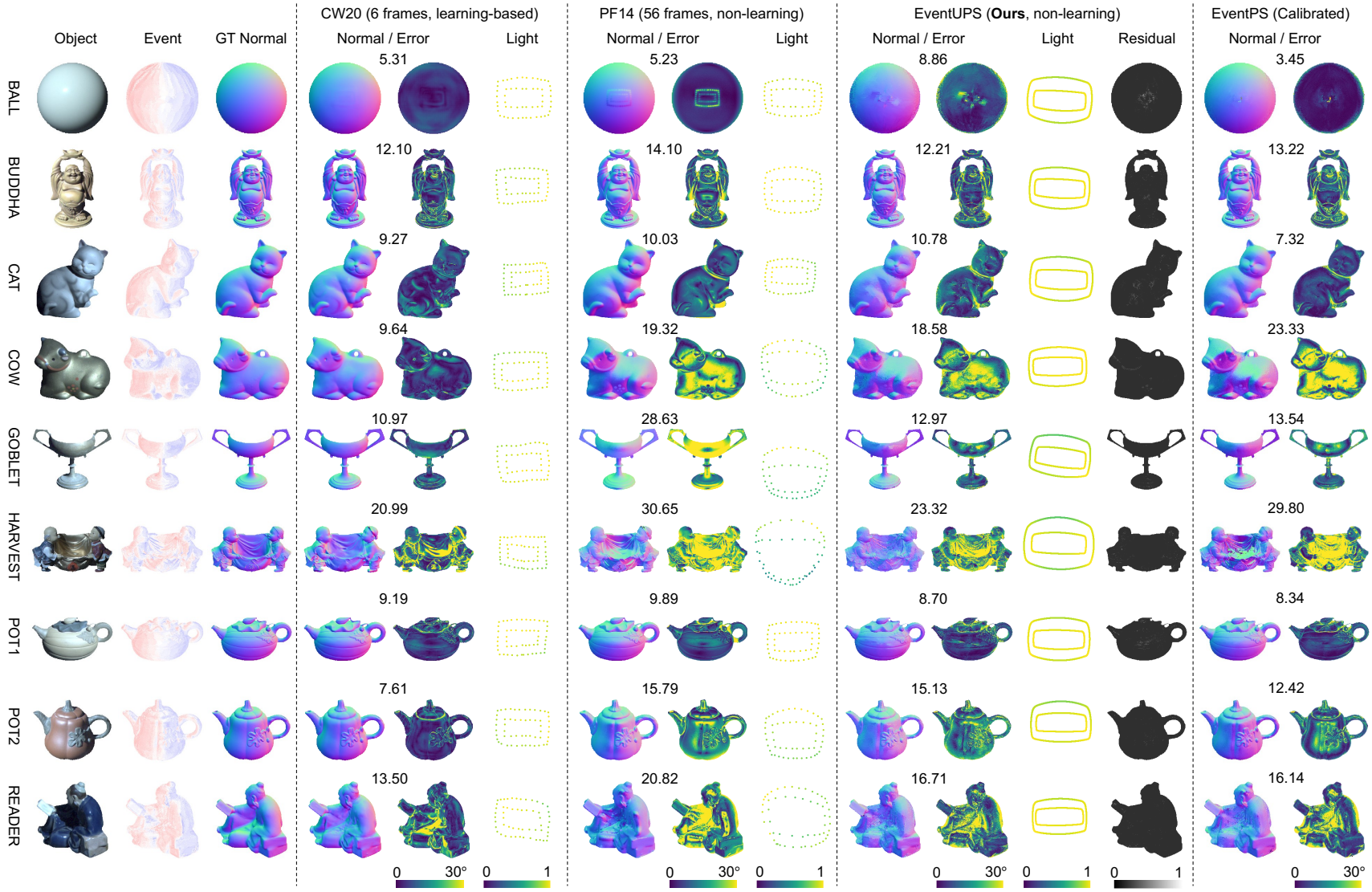

Figure 14. Complete visual results on the DiLiGenT-Ev semi-real dataset, showing the full set of reconstructions for all objects.